

# Seeing the trees in the forest when estimating riparian shade

Kevin R. Gehring, Ph.D.  
Biometrics Northwest LLC  
Redmond, WA  
Email: krg@biometricsnw.com

## Abstract

Riparian forest management is impacted by requirements to provide stream shading. Models of riparian shading assume a simple opaque wall of trees adjacent to a stream, the “view to sky” model, or uniform light transmission properties for the forest canopy and understory adjacent to a stream. These approaches fail to recognize the discrete nature of the trees within a riparian forest, including gaps and opaque boles. Advances in desktop computing power allow the estimation of shade using individual trees in a riparian forest. A potential shade model was implemented using ray tracing within a bootstrap simulation framework to approximate the distribution of stream shading that could be provided by a riparian forest. The view to sky shade model, the uniform property shade model, and an individual tree shade model are compared using two management scenarios to identify strengths and weaknesses of the three shade modeling approaches.

**Key Words:** Shade, ray tracing, bootstrap simulation, riparian forest management

## 1 Introduction

Shade requirements for streams are typically included in riparian forest management rules. Two common shade modeling approaches are the view to sky model (Sullivan et al., 1990) and the use of uniform property slabs to represent the features of a riparian forest. The view to sky model assumes an opaque wall of trees adjacent to a stream, and the uniform property slabs approach assumes uniform light transmission and other properties for large volumes representing the canopy and understory of a forest adjacent to a stream. These two approaches fail to recognize the discrete nature of trees in a forest, canopy gaps, opaque boles, and tree locations that can significantly impact the amount of shade reaching a stream. Modern desktop computing power makes it feasible to use an individual tree shade model to identify differences between the performance of the individual tree model and the view to sky and uniform property slab models to investigate potential impacts that could affect riparian forest management decisions.

The impetus to perform this comparison was inspired by a desire to understand the differences among these three shade modeling approaches, with regard to their limitations and their benefits. A significant factor in motivating this work was the uncritical manner in which several biologists in a meeting were discussing different approaches to estimating shade in the context of developing riparian management measures for a habitat conservation plan. There was apparent confusion between canopy cover, measured vertically, and canopy closure, measured using angles of view (Korhonen et al., 2006, Fiala et al., 2006), and between the use of vertical canopy density a measure consistent with canopy cover, and angular canopy density (Brazier and Brown, 1973), a measurement consistent with canopy closure.

### 1.1 Objectives

Compare the view to sky shade model, the uniform property slab shade model, and an individual tree shade model for a simulated riparian forest. The three shade models will be compared by using ray-tracing to model light transmission through the riparian forests to the center of a stream within a bootstrap simulation framework to estimate variability. A management scenario having a 50 foot no harvest buffer with a 50 year rotation and a no action scenario will be used to identify strengths and weaknesses of the three shade modeling approaches.

## 2 Methods

The shade modeling approaches described below have been implemented as a post processor for a multi-zone managed riparian buffer simulation system (Gehring, 2008) that uses bootstrap simulations (Efron, 1982, Efron and Tibshirani, 1998) to approximate distributions of stand attributes.

## 2.1 Ray tracing shade models

The approach used here to implement the shade models follows closely the approach used for the riparian aquatic interaction simulator (RAIS) model (Welty et al., 2002). The RAIS model computes an estimate of potential blocking for a point located in the center of a stream rather than solar shade for simplicity. Potential blocking computes the ratio of total obstructed light intensity to total unobstructed light intensity at a specific point located in the center of a stream to determine the proportion of the total possible light that reaches the point, and then subtracts this value from one to obtain the blocking effect, or shading. Using potential blocking simplifies the process of estimating shading by eliminating the need to include latitude, stream orientation, and the position of the sun, to compute solar derived shading, while providing an effective tool for making relative comparisons among management scenarios for riparian forests or as a shading index to compare different forest structures.

The potential blocking shade model assumes the Beer-Lambert Law of light transmission through a medium. The Beer-Lambert Law is defined by the equation  $I = I_0 \lambda^L$ , where  $I$  is transmitted light intensity,  $I_0$  is incident light intensity,  $\lambda$  is the attenuation coefficient giving the amount of light intensity remaining after one unit of travel through a particular medium, and  $L$  is the path length through the medium. The total attenuation for a light ray passing through  $n$  objects  $O_1, O_2, \dots, O_n$  having attenuation coefficients  $\lambda_1, \lambda_2, \dots, \lambda_n$  and path lengths through the objects of  $L_1, L_2, \dots, L_n$  is given by the product of the attenuation values for each object  $\lambda_1^{L_1} \times \lambda_2^{L_2} \times \dots \times \lambda_n^{L_n}$ , yielding the formula

$$I = I_0 \lambda_1^{L_1} \times \lambda_2^{L_2} \times \dots \times \lambda_n^{L_n}.$$

Light intensity or incident energy varies by azimuth, or angle above the horizon  $\beta$ , with the maximum light intensity from directly overhead,  $\beta = 90^\circ$  or  $\beta = \frac{\pi}{2}$  radians, and the minimum light intensity of zero at the surface,  $\beta = 0$  degrees or radians. A sinusoidal profile was assumed for the initial light intensity or incident energy, based on angle above the horizon  $\beta$ ,  $I_0(\beta) = \sin(\beta)$ .

Potential blocking for a point in the center of the stream is computed in two passes by first integrating the initial light intensity  $I_0(\theta, \beta)$  over the hemisphere defined by the angles  $\theta \in [0^\circ, 360^\circ)$ , or  $\theta \in [0, 2\pi)$  radians, and the azimuth  $\beta$ , located over the point to obtain the total unobstructed light intensity  $T_u$ ,

$$T_u = \int_0^{2\pi} \int_0^{\frac{\pi}{2}} I_0(\theta, \beta) d\beta d\theta$$

and then integrating the transmitted light intensity  $I(\theta, \beta)$  computed using the Beer-Lambert Law with the riparian forest present over the hemisphere in the same manner to obtain the total obstructed light intensity  $T_o$ . The potential blocking  $B$  is then

$$B = 1 - \frac{T_o}{T_u}$$

which represents the proportion of the total light intensity that was blocked by the riparian forest. Multiplying  $B$  by 100 converts the value to a blocking or shading percent.

Table 1: Light attenuation coefficients for Beer-Lambert Law of light transmission. These values give the amount of the incident light that is left after travelling one foot through a particular medium.

Medium	Attenuation coefficient
Forest canopy	0.95 per foot
Under canopy	0.99 per foot
Tree crown	0.95 per foot
Tree bole	0.00 per foot
Shrub Layer	0.84 per foot

The integrals allow a clean, concise definition of the formulas used to compute potential blocking, but to implement the procedures on a computer a discretization of the problem is necessary. The discretized algorithm computes potential blocking for a point in the center of the stream by using  $N$  uniformly distributed points  $p_i$  representing equal surface areas on a unit hemisphere (Leopardi, 2006) located over the point in the center of the stream to direct rays  $r_i$  that pass through the points  $p_i$  on the hemisphere into the surrounding space. The two integrals then become sums over the  $N$  rays  $r_i$  that compute an approximation  $\hat{T}_u$  to the total unobstructed light intensity

$$\hat{T}_u = \sum_{i=1}^N I_0(r_i) = \sum_{i=1}^N I_0(\theta_i, \beta_i)$$

and, similarly for  $\hat{T}_o$  and the total obstructed light intensity at the point in the center of the stream, where  $I_0(r_i)$  is the initial light intensity for the ray  $r_i$ , which can be represented as the point  $(\theta_i, \beta_i)$  in spherical coordinates via a straightforward transformation (Silas and Hille, 1982). The formula

$$\hat{B} = 1 - \frac{\hat{T}_o}{\hat{T}_u}$$

is then used to obtain the approximate value for the potential blocking for the point in the center of the stream. The rays  $r_i$  derived from  $N = 2500$  points  $p_i$  on the unit hemisphere are shown in Figure 1. These rays were used for all of the potential blocking simulations.

To use the Beer-Lambert Law light attenuation coefficients  $\lambda$  are necessary for each type of media that a light ray can intersect. The media that occur in the riparian shade simulations represent different characteristics of the riparian forest, and are listed in Table 1. The attenuation coefficients for the forest canopy and the shrub layer are from (Welty et al., 2002). The under canopy attenuation coefficient was assigned the value 0.99 since light transmission under the canopy is not perfect. The attenuation coefficient for the tree bole is obvious, tree boles are opaque and do not transmit light, and the tree crown attenuation coefficient was given the same value as that for the forest canopy, for lack of a better value to use.

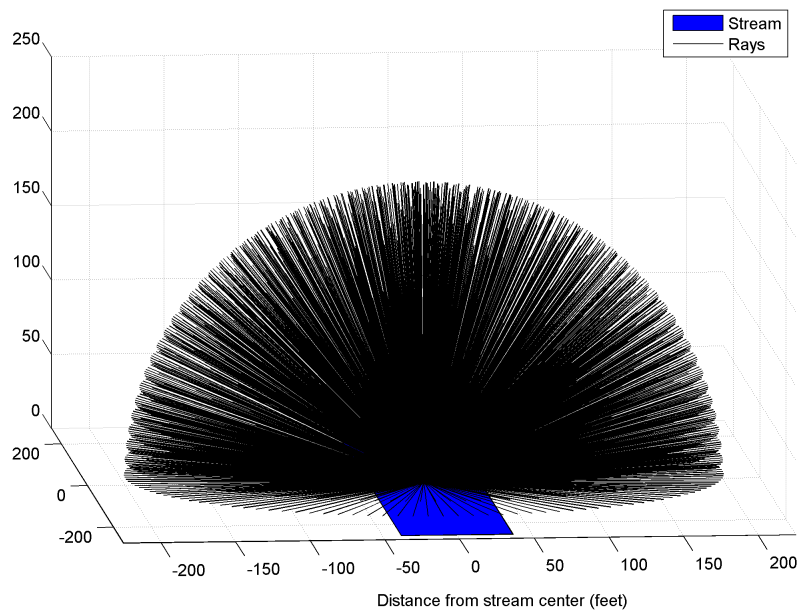


Figure 1: Rays used for shade/blocking ray tracing for all shade models.

## 2.2 Riparian simulation area

The riparian area of interest for the shade model comparisons was assumed to be a relatively flat, four acre riparian management zone (RMZ) located immediately adjacent to a stream, with two one acre forest stands located adjacent to each other across the stream and parallel to the stream on each side. The RMZ was assumed to have a width of 170 feet on both sides of the stream, measured perpendicular or up slope to the stream, and a total stream reach of 512 feet, measured along the bank of the stream. The origin, or (0,0) point, for the riparian simulation area was located at the intersection of the centerline of the stream and the perpendicular line between the two one acre forest stands on each side of the stream. The value of 170 feet for the buffer width was chosen based on the total width of a riparian buffer that would be required under the Forests and Fish Law of Washington State (WFPB, 2001) for productive Douglas-fir (*Pseudotsuga menziesii*) stands in site class II (King, 1966).

Two stream sizes were used for the comparison to investigate differences in the amount of shading that occur at the center of large and small streams. The large stream was assumed to have a 75 foot bankfull width and the small stream a bankfull width of 5 feet.

### 2.2.1 View to Sky shade model

The view to sky shade model (Sullivan et al., 1990) assumes that the riparian forests adjacent to a stream form opaque walls that do not transmit light. The height of the wall is based on the height  $H$  of the trees in the riparian forest adjacent to the stream, and the height is usually reduced by converting it into an effective height  $H_E$  using an estimated value of opacity to account for the more open conditions in the upper canopy, particularly in conifer forests with pointed tree tops and large gaps between them. The opacity estimate is usually derived from vertical canopy opacity. The view to sky wall may be placed directly adjacent to the stream or set back from it, depending on the specific conditions and the objectives of an analysis.

For this comparison, the view to sky walls were located directly adjacent to a stream, and the effective height was assumed to be 80% of the mean height of the trees in a 50 foot wide no harvest region also directly adjacent to the stream.

### 2.2.2 Uniform property slab shade model

The uniform property slab shade model assumes that the riparian forest can be decomposed into large, rectangular slabs having uniform light transmission properties. The decomposition into slabs is performed based on identified subzones within a riparian forest having different characteristics. Three types of slabs are recognized, a slab representing a forest canopy layer, a slab representing an under-canopy layer, and a slab for a shrub layer. Each type of slab has different light transmission characteristics as specified by the Beer-Lambert Law attenuation coefficients in Table 1. The slabs for the zone directly adjacent to the stream begin at the stream edge.

For this comparison, the slabs representing the different components of the riparian forest were defined using upper and lower limits to specify the vertical extent of the slab for each subzone. The most important slabs are those for the forest canopy, and they were defined by specifying upper and lower canopy levels based on the heights and height to

the base of the live crowns of the trees in the riparian forest. The upper canopy level was computed by taking the mean height of all of the trees within a subzone, and the lower canopy level was computed by averaging the minimum and median values for height to the base of the live crown for each subzone. The top of the under-canopy slab was equal to the lower canopy level for each subzone, and the bottom of the under-canopy slab was either the ground, at a height of zero, the top of a five foot tall shrub layer. A shrub layer was present only if the lower canopy level was at least 10 feet high.

### **2.2.3 Individual tree shade model**

The individual tree shade model represents the riparian forest using individual trees comprised of opaque rectangular boles and rectangular crowns. The bole of the tree was assumed to stop at the bottom of the crown. Rectangular shapes were used for speed of computation, ray-plane intersections being very fast, and should provide a very reasonable approximation to the light transmission characteristics of an actual forest.

For this comparison, the rectangular crowns were inscribed within the circle defined by the crown radius centered on the tree and had upper and lower limits defined by the tree height and the height to the live crown base. The tree boles were inscribed within the circle defined by the diameter at breast height centered on the tree. A five foot high slab based shrub layer was present for this shade model if the lower canopy level was at least 10 feet high.

## **2.3 Management scenario descriptions**

Two management scenarios are compared to identify strengths and weaknesses of the three shade models. A 160 year time horizon was used when running the forest growth model projections. The forest growth model used was SMC-ORGANON version 8.2, an updated version of the SMC-ORGANON model (Hann et al., 1997, Hanus et al., 1999, Hann et al., 2003, 2006) calibrated using the forest inventory database of the Stand Management Cooperative (Chappell et al., 1988).

Two management options were used to populate the management scenarios with trees. Tree lists for each of the management options described below were based on the SMC-ORGANON model projections with five year output intervals obtained using an initial tree list representing an actual, 20 year old riparian stand, the base stand. The base stand is a 100% pure stand of Douglas-fir, that contained 471 standing, live Douglas-fir trees per acre, located in south-western Washington State. The base stand had a site index of 120 ft at 50 years and was a Douglas-fir site class II stand (King, 1966). The trees in the base stand had a mean DBH of 7.4 inches, with a standard deviation of 1.9 inches and a range from 4.0 inches to 13.0 inches, a mean height of 48.5 ft, with a standard deviation of 3.9 ft and a range from 43.0 ft to 67.0 ft. This stand structure was considered to be representative of the young, relatively dense riparian forest stands that dominate the managed riparian areas in western Washington, and was chosen as the base stand for the management option projections for this reason. All of the management options were assumed to represent a one acre riparian buffer area with Douglas-fir site class II and a 50 year site index of 120 ft (King, 1966). The SMC-ORGANON model projections were performed using internal height

and diameter growth calibrations that adjust the model to the account for the initial tree dimensions, site index, and age. No other model calibrations were performed.

The management option descriptions appear in the list below. In the management option descriptions a commercial thinning is denoted by CT and represents a thinning operation producing sufficient merchantable material to at least offset the cost of the thinning operation. Thinning from below removes the smallest diameter trees first and was the only type of thinning operation considered. For each management option the complete set of management operations over the 160 year time horizon are included.

**NOACTION** Plant 471 TPA and grow with no thinning.

**UPLAND** Plant 471 TPA. CT to 180 TPA from below at age 20. CT to 100 TPA from below at age 35. Clearcut at age 50, leaving 2 TPA at least 20 inches DBH and another 2 TPA at least 12 inches DBH. Plant 300 TPA. CT to 180 TPA from below at age 70. CT to 100 TPA from below at age 85. Clearcut at age 100, leaving the 4 largest TPA. Plant 300 TPA. CT to 180 TPA from below at age 120. CT to 100 TPA from below at age 135. Clearcut at age 150, leaving the four largest TPA. Plant 300 TPA.

Descriptions of the two management scenarios, their respective management zones, and the assigned management options appear below. The management scenarios were generated using a multi-zone managed riparian buffer simulation system (Gehring, 2008) that uses bootstrap simulations (Efron, 1982, Efron and Tibshirani, 1998) to approximate distributions of stand attributes for each management scenario and output year using the management option tree lists generated by a forest growth model. The bootstrap simulations randomly selected and placed trees within a riparian management subzone proportionally using tree lists from the management option assigned to that subzone. A uniform, distribution of tree locations was assumed within each defined management zone, and only trees having diameter at breast height values of at least four inches were used.

The shade model comparisons used tree lists from each management scenario and output time to populate the four one acre areas adjacent to a stream that comprise the simulated riparian forest area described in Section 2.2. A total of 25 bootstrap simulations were generated for each management scenario and used to compute mean values and standard deviations for shade trajectories over time.

**50 ft No Harvest** This management scenario represents a baseline 50 ft no harvest zone with a 50 year rotation and has two subzones. The first subzone is assigned the NOACTION management option and ranges from 0 ft to 50 ft from a stream. The second subzone is assigned the UPLAND management option and ranges from 50 ft to 170 ft from a stream.

**No Action** This management scenario represents the no action baseline of an unmanaged forest and has a single zone, which is assigned the NOACTION management option from 0 ft to 170 ft.



### 3 Results and discussion

Results of the shade simulations are presented graphically as a pair of figures for each stream size. The first of the figures shows actual scale 3-D visualizations of the stream at an age of 80 years, with the view to sky walls, the forest slabs, and the individual trees used for each of the shade simulations. The second figure shows shading over time with 95% bootstrap confidence intervals for the mean shading values computed using the Student's  $t$ -distribution with  $t_{0.975} = 2.0639$  and  $\nu = 24$  degrees of freedom. In the figures for the management scenario visualizations, the 50 ft No Harvest management scenario is on the left and the No Action management scenario is on the right. The view to sky shade model is represented in the top row, with the uniform property slab shade model in the middle row, and the individual tree shade model in the bottom row. The unit hemisphere directing the rays through the forest would be located at the intersection of the two zero lines located on the "ground". The figures for the shading over time have the same top-to-bottom arrangement of shade models but display curves for both management scenarios concurrently to facilitate their direct comparison.

Visualizations for the small stream size are shown in Figure 2 and plots of shading over time are shown in Figure 3. The stream is located at the zero point in the center front and is not readily visible in the view to sky and individual tree visualizations, but it is visible in the uniform property slabs visualization. The shading plots over time tell the story.

For the small stream, the view to sky shade model did not distinguish between the two management scenarios whose trajectories overlap. The shading percent starts at approximately 93.5% for both scenarios and approaches a value of 98.1% by an age of 160 years, and there is virtually no variability, with the 95% confidence intervals barely discernible.

The uniform property slabs shade model did distinguish between the two management scenarios, clearly indicating a decline of approximately 6 percentage points in shading after the harvests at 50, 100, and 150 years. An almost complete recovery to the No Action shading level just prior the second harvest was also present, but the recovery from the second to the third harvest, while peaking at the same level as before, was further from the No Action shading level at that age, evidenced by the wider gap. Both of the management scenarios had initial shade levels of 87%, with the No Action scenario approaching a value of 97.5% by age 160 and the 50 ft No Harvest scenario cycling between 88% after harvest to a value of 94% just prior to the next harvest. Variability was, again, quite low.

The individual tree shade model also distinguished between the two management scenarios, clearly indicating declines after the harvest events and indicating a much higher degree of variability than the other two shade models. The post-harvest declines were approximately 5, 6, and 7 percentage points to values of 78%, 75%, and 72%, respectively, with the increase most likely caused by mortality within the 50 foot no harvest zone adjacent to the stream. Post-harvest recovery of the shading levels achieved 81% after the first harvest and 79.5% after the second harvest, and are likely also declining due to mortality within the 50 foot no harvest zone. The initial shade level for the 50 ft No Harvest scenario was approximately 68%, after which the the shade levels cycled between their post-harvest lows and pre-harvest highs. The initial shade level for the No Action scenario was approximately 71%, and the shade trajectory approached a level that fluctuated between 86% and 88%. Differences in the initial shade levels were small, and may due to the initial thinning event

in the 50 year rotation zone, or just random variability due to differences in tree locations. The fluctuations in the shade levels for the No Action scenario were a result of the combined effects of tree locations and mortality. Note the drop of 10 percentage points in the shade levels when individual trees are taken into account, indicating that gaps between tree crowns reduce the maximum obtainable level of shading.

Visualizations for the large stream size are shown in Figure 4 and plots of shading over time are shown in Figure 5. The stream is located at the zero point in the center front and is readily visible in the visualizations for the three shade model simulations and two management scenarios. Again, the shading plots over time tell the story, which is essentially identical to the story for the small streams, so only the highlights are presented.

The view to sky shade model did not distinguish between the management scenarios. Initial shade levels for both scenarios were approximately 30% and they approached a value of approximately 73% by an age of 160 years.

The uniform property slabs shade model did distinguish between the two management scenarios, clearly indicating the decline after each harvest event and the subsequent recovery for the 50 ft No Harvest scenario. The post-harvest declines were 7, 11, 9 percentage points for the three harvest events with recoveries to approximately 67% after the first harvest and 69% after the second harvest. The initial shade levels for both management scenarios were 29.6%, and the No Action scenario was approaching a shade level of 74% by an age of 160 years. The small increase in shade level, 2 percentage points, between the two post harvest recovery levels may be attributable to blocking caused by the forest canopy slab for the 50 year rotation zone.

The individual tree shade model also clearly distinguished between the two management scenarios, clearly indicating post-harvest declines and indicating a much higher degree of variability than the other two shade models. The post-harvest declines were approximately 8, 11, and 11 percentage points to values of 42%, 44%, and 44%, respectively. Post-harvest recovery of the shading levels achieved 55% after the first and second harvest events. The initial shade level for the 50 ft No Harvest scenario was approximately 25%, after which the the shade levels cycled between their post-harvest lows and pre-harvest highs. The initial shade level for the No Action scenario was approximately 26%, and the shade trajectory approached a level that fluctuated between 61% and 64%. Differences in the initial shade levels were very small, and may be due to the initial thinning event in the 50 year rotation zone, or just random variability due to differences in tree locations. The fluctuations in the shade levels for the No Action scenario were a result of the combined effects of tree locations and mortality. Note the drop of 10 to 16 percentage points in the shade levels when individual trees are taken into account, indicating that gaps between tree crowns reduce the maximum obtainable level of shading.

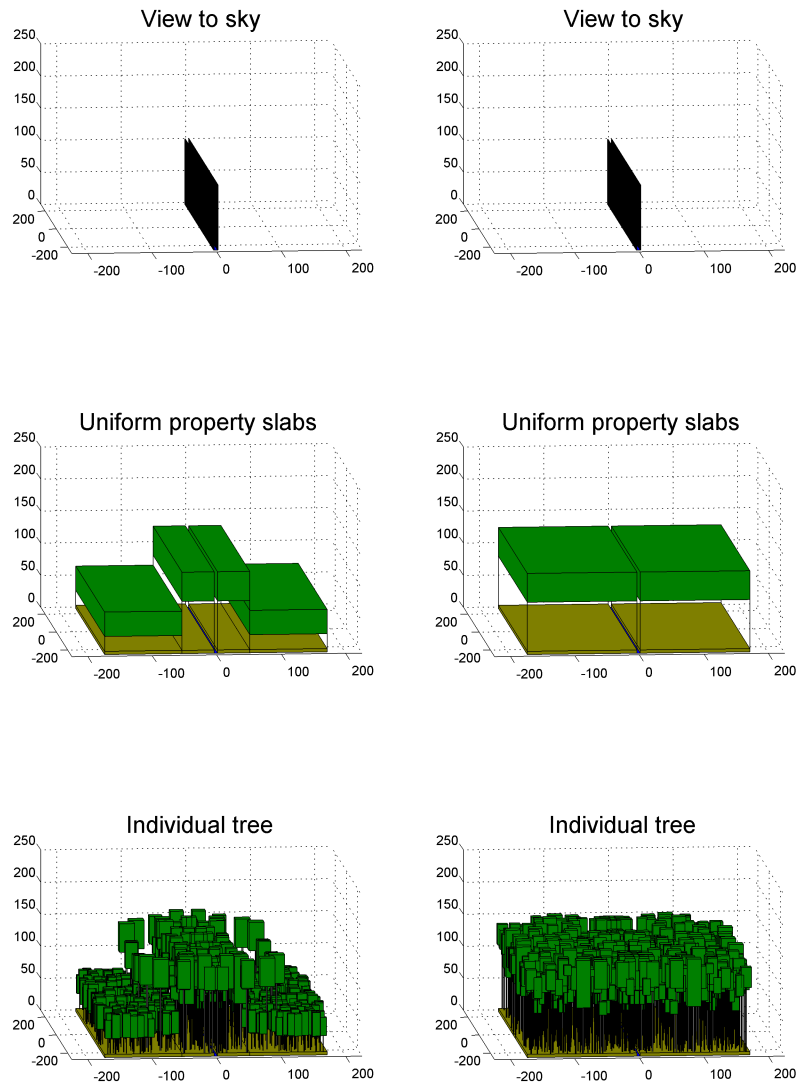


Figure 2: Small stream shade model visualizations for the two management scenarios.

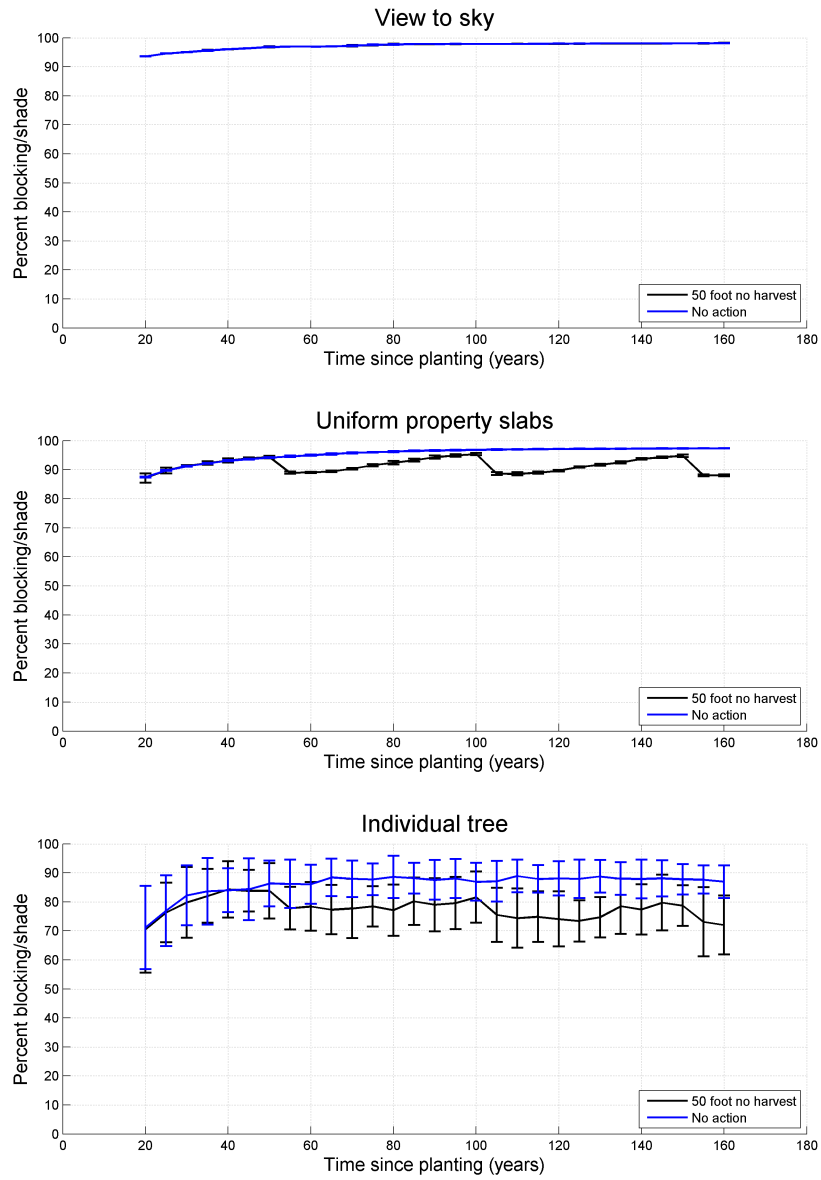


Figure 3: Small stream shade model results for the two management scenarios.

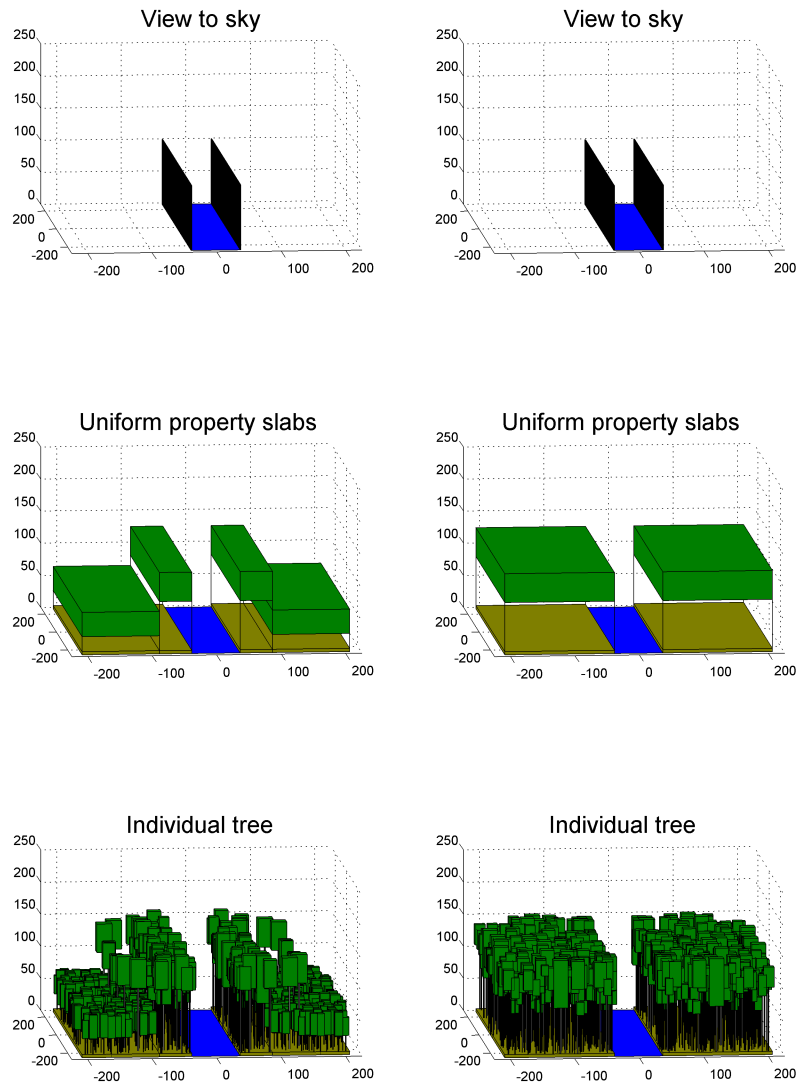


Figure 4: Large stream shade model visualizations for the two management scenarios.

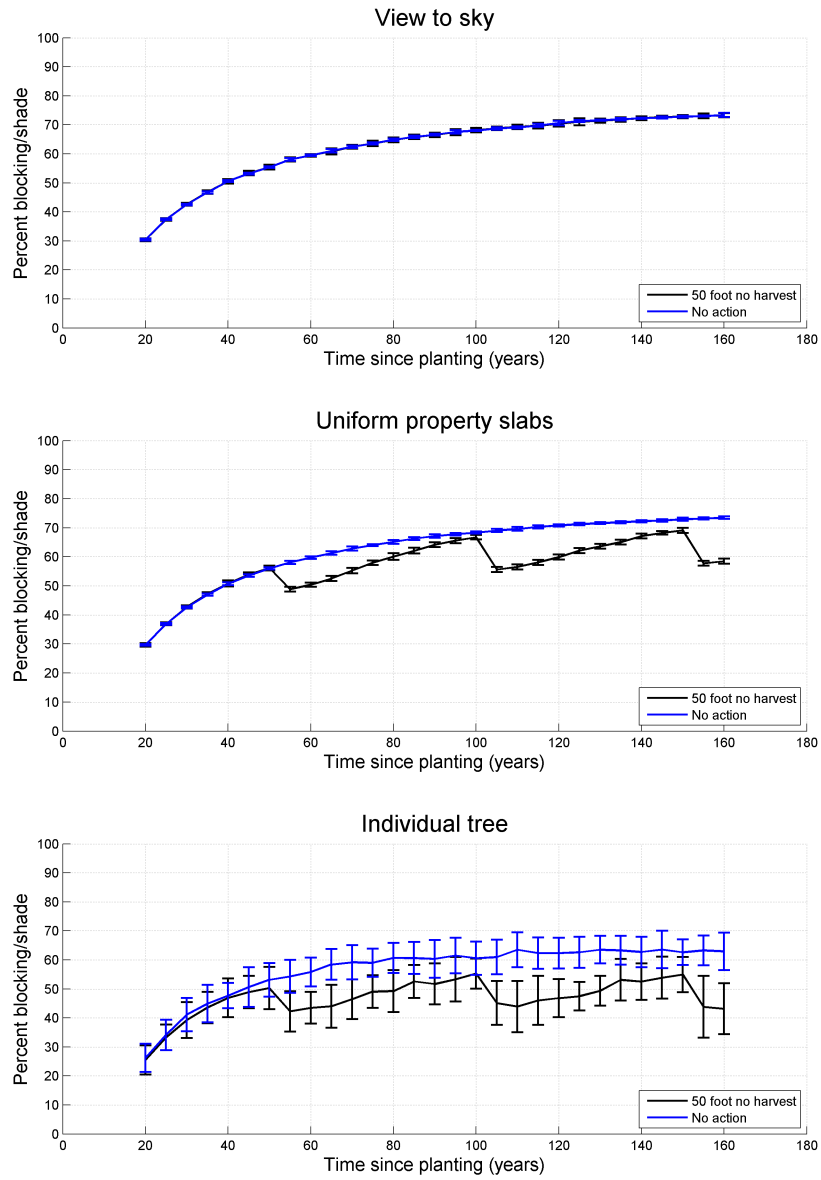


Figure 5: Large stream shade model results for the two management scenarios.

## 4 Conclusions

The comparison just performed clearly identified strengths and weakness among the three shade model simulation approaches. First, the view to sky approach is not useful for making relative comparisons among management scenarios since it does not distinguish between management scenarios, but may be useful for obtaining rough estimates of shading for unmanaged forests. Second, the uniform property slabs approach allows relative comparisons among management scenarios but underestimates variability due to long path lengths through the slabs representing the riparian forest. Third, the view to sky and uniform property slab approaches both overestimate blocking/shade relative to the individual tree approach, indicating that some care should be used when comparing shading computed using these methods with actual ground estimates of shading. Fourth, the individual tree approach clearly distinguished between management scenarios and demonstrated the influence of the discrete nature of trees through the increased level of variability. Finally, if it is important to distinguish among the shading levels provided by different riparian forest management scenarios, then the uniform property slabs shade model is the minimum level of resolution that must be used, and if tree location is important, then the individual tree model should be used.

## Literature Cited

- Brazier, J. R. and G. W. Brown (1973, April). Buffer strips for stream temperature control. Research Paper 15, Forest Research Laboratory, Oregon State University, Corvallis, Oregon.
- Chappell, H. N., R. O. Curtis, D. M. Hyink, and D. A. Maguire (1988, 23-27 August). The Pacific Northwest stand management cooperative and its field installation design. In *Forest Growth Modelling and Prediction, Proceedings of the IUFRO Conference*, Volume NC-120 of *USDA For. Serv. Gen. Tech. Rep.*, Minneapolis, Minn., pp. 1073–1080.
- Efron, B. (1982). *The jackknife, the bootstrap and other resampling plans*. CBMS-NSF Regional Conference Series in Applied Mathematics 38. SIAM.
- Efron, B. and R. J. Tibshirani (1998). *An Introduction to the Bootstrap*. Monographs on Statistics and Applied Probability 57. Chapman & Hall/CRC.
- Fiala, A. C., S. L. Garman, and A. N. Gray (2006). Comparison of five canopy cover estimation techniques in the western Oregon Cascades. *Forest Ecology and Management* 232, 188–197.
- Gehringer, K. R. (2008). An individual tree simulation model for multi-zone managed riparian buffers (DRAFT). Technical report, Biometrics Northwest LLC, Redmond, Washington.  
[http://www.biometricsnw.com/projects/ripariansim/workingpaper\\_managedbuffers.pdf](http://www.biometricsnw.com/projects/ripariansim/workingpaper_managedbuffers.pdf).
- Hann, D., A. Hester, and C. Olsen (1997). *ORGANON User's manual Edition 6.0*. Corvallis, Oregon: Forest Research Lab, Oregon State University.

- Hann, D. W., D. D. Marshall, and M. L. Hanus (2003). Equations for predicting height-to-crown-base, 5-year diameter-growth rate, 5-year height-growth rate, 5-year mortality rate, and maximum size-density trajectory for douglas-fir and western hemlock in the coastal region of the pacific northwest. Technical report, Forest Research Lab, Oregon State University, Corvallis, Oregon. Research Contribution 40. 83p.
- Hann, D. W., D. D. Marshall, and M. L. Hanus (2006). Re-analysis of the SMC-ORGANON equations for diameter-growth rate, height-growth rate, and mortality rate equations of douglas-fir. Technical report, Forest Research Lab, Oregon State University, Corvallis, Oregon. Research Contribution 49. 24p.
- Hanus, M. L., D. D. Marshall, and D. W. Hann (1999). Height-diameter equations for six species in the coastal regions of the pacific northwest. Technical report, Forest Research Lab, Oregon State University, Corvallis, Oregon. Research Contribution 25. 11p.
- King, J. E. (1966, July). *Site index curves of Douglas-fir in the Pacific Northwest*. Number 8 in Weyerhaeuser Forestry Paper. Weyerhaeuser Company.
- Korhonen, L., K. T. Korhonen, M. Rautiainen, and P. Stenberg (2006). Estimation of forest canopy cover: a comparison of field measurement techniques. *Silva Fennica* 40(4), 577–588.
- Leopardi, P. (2006). A partition of the unit sphere into regions of equal area and small diameter. *Electronic Transactions on Numerical Analysis* 25, 309–327. ISSN 1068-9613.
- Silas, S. and E. Hille (1982). *Calculus: One and several variables with analytic geometry* (Fourth ed.). John Wiley and Sons.
- Sullivan, K., J. Tooley, K. Doughty, J. E. Caldwell, and P. Knudsen (1990). Evaluation of prediction models and characterization of stream temperature regimes in Washington. Timber/Fish/Wildlife Report No. TFW-WQ3-90-006, Washington Department of Natural Resources, Olympia, Washington.
- Welty, J. J., T. Beechie, K. Sullivan, D. M. Hyink, R. E. Bilby, C. Andrus, and G. Pess (2002). Riparian aquatic interaction simulator (RAIS): a model of riparian forest dynamics for the generation of large woody debris and shade. *Forest Ecology and Management* 162, 299–318.
- WFPB (2001). *Forest Practices Rule Book*. Olympia, Washington: Washington Forest Practices Board, Washington Department of Natural Resources. Forest Practices Division.